NASA TECHNICAL MEMORANDUM

NASA TM X-72772

NASA TM X-72772

(NASA-TM-X-72772) WIND TUNNEL BLOCKAGE TESTS AT MACH 5 OF VACUUM DUCT MODELS FOR TWO SOUND RADIATION SHIELDS (NASA) 29 p HC $4.00 CSCL 14B

N76-32201

G3/09 Unclas C4079

WIND TUNNEL BLOCKAGE TESTS AT MACH 5 OF VACUUM DUCT MODELS FOR TWO SOUND RADIATION SHIELDS

BY IVAN E. BECKWITH AND WILLIAM D. HARVEY

September 1975

This informal documentation medium is used to provide accelerated or special release of technical information to selected users. The contents may not meet NASA formal editing and publication standards, may be revised, or may be incorporated in another publication.

NATIONAL AERONAUTICS AND SPACE ADMINISTRATION
LANGLEY RESEARCH CENTER, HAMPTON, VIRGINIA 23665

1. Report No.	2. Government Accession No.	3. Recipient's Catalog No.
NASA TM X- 72772		

4. Title and Subtitle	5. Report Date
Wind Tunnel Blockage Tests at Mach 5 of Vacuum Duct Models For Two Sound Radiation Shields	September 1975
	6. Performing Organization Code 37.210

7. Author(s)	8. Performing Organization Report No.
Ivan E. Beckwith and William D. Harvey	

9. Performing Organization Name and Address	10. Work Unit No.
NASA Langley Research Center Hampton, VA 23665	505-06-41-01
	11. Contract or Grant No.
	13. Type of Report and Period Covered Technical Memorandum
12. Sponsoring Agency Name and Address National Aeronautics and Space Administration Washington, DC 20546	14. Sponsoring Agency Code

15. Supplementary Notes

Preliminary release of special information which may be included in formal NASA reports.

16. Abstract

Two sound shield models with dummy vacuum exhaust ducts have been tested in the Langley Mach 5 Pilot Quiet Tunnel. The first model simulates a new sound shield of 3 in. (7.62 cm) inside diameter and the second model is a shield of 4 in. (10.16 cm) inside diameter. The dummy vacuum exhaust ducts were attached to the external housing of the models. The flow in the first model, which had a by-pass mass flow ratio of about 0.6, could not be started except at the two highest test Reynolds numbers where only the central core flow region was started. The flow in the second model with a mass ratio of approximately 0.3 was fully started except at the lowest unit Reynolds number where some unsteadiness and partial flow separation at the wall was observed. Since the external housing and dummy vacuum ducts were the same for both models, these results indicate that the ratio of by-pass mass flow to total mass flow for a wind tunnel sound shield of this particular design must be less than about 0.3. Hence, a lower limit is imposed on the inlet diameter of the sound shield in relation to the exit diameter of the wind tunnel nozzle. This lower limit on the inlet diameter may possibly be reduced by improvements in streamlining of the external housing and ducts, by reductions in blockage area, or by the use of external ducting shrouds; however, such modifications have not yet been tested.

17. Key Words (Suggested by Author(s))	18. Distribution Statement
Supersonic Wind Tunnels flow blockage sound shields .09 Research and Support Facilities (Air)	Unclassified Unlimited

19. Security Classif. (of this report)	20. Security Classif. (of this page)	21. No. of Pages	22. Price*
Unclassified	Unclassified	28	$3.75

*For sale by the National Technical Information Service, Springfield, Virginia 22161

Wind Tunnel Blockage Tests at Mach 5 of Vacuum Duct Models For Two Sound Radiation Shields

By Ivan E. Beckwith and William D. Harvey

Langley Research Center

SUMMARY

Two sound shield models with dummy vacuum exhaust ducts have been tested for wind tunnel flow blockage at Mach 5 over a free-stream unit Reynolds number range from about 2.5 x 10^6 per ft (8.2 x 10^6 per m) to 14 x 10^6 per ft. (45.9 x 10^6 per m). Each model was fitted with four ducts that had sharp leading edges swept back 63° with respect to the free-stream nozzle flow. The ducts are 4 in. (10.16 cm) wide and simulate the external blockage area of the actual plenum suction ducts which will have an internal cross-sectional flow area of approximately 20.5 in.^{2} (132.3 cm^2) each.

The first model consisted of a solid wall, sharp leading edge cylinder of 3 in. (7.62 cm) inside diameter inserted into the external housing and ducting assembly that was used for both models. The second model is the 4 in.(10.16 cm) inside diameter sound shield model tested previously. The inside wall of this model consists of a cylindrical array of nearly parallel rods.

The flow in the first model was not "started" (the internal flow is considered fully "started" when it is nearly uniform throughout at the desired supersonic Mach number) except at the two highest unit Reynolds numbers where only the central region of the core flow at the exit was started. The internal flow in the second model was fully started except at the lowest unit Reynolds number where some unsteadiness of the flow at the core edges was observed.

The ratios of the by-pass mass flow to the total flow was about 0.6 and 0.3 for the first and second models, respectively. Hence, it is concluded

that to insure fully started flow over the whole range of Reynolds number for a rod wall wind tunnel sound shield with ducts similar to those tested, the bypass mass flow ratio must be somewhat smaller than 0.3. This result imposes a lower limit on the inside diameter of the sound shield in relation to the wind tunnel nozzle exit diameter. This limiting diameter might be further reduced by improvements in the streamlining and by reductions in blockage area of the external housing and ducts, or by the use of an external shroud, but such modifications have not yet been tested.

INTRODUCTION

The high free-stream noise levels in wind tunnels at Mach numbers greater than about 2.5 consist primarily of sound radiated from the turbulent boundary layers on the nozzle walls (refs. 1 to 4). Test results from conceptual planar models of a rod wall sound shield show that these noise levels can be reduced significantly when the boundary layers on the rods are maintained laminar (refs. 5 to 9). This type of sound shield consists of an array of small diameter rods aligned with the flow and with narrow gaps between the rods for boundary layer removal and laminarization by suction.

Results of preliminary tests at Mach 5 of a small axisymmetric sound shield with 1/4 in. (0.635 cm) diameter rods showed that no sound attenuation was obtained at Reynolds numbers above 3.5×10^6 per ft (11.5×10^6 per m) because of premature transition of the rod boundary layers and insufficient suction mass flow (ref. 10). The ratio of the minimum gap width to rod diameter (g/d) was 0.068 for these tests.

Data reported in references 8 and 9 showed that the local transition Reynolds number at the end of a 2 ft (0.61 m) long flat shield was 7×10^6 for g/d = 0.12 and 14×10^6 for g/d = 0.16. Application of these results to the

15 in. (38.1 cm) long axisymmetric shield of reference 10 indicated that the length transition Reynolds number would be increased to about 6×10^6 and 9×10^6 by increasing g/d to 0.12 and 0.16, respectively, if the inviscid cross-flow suction velocity at the gaps is sonic (this component of the suction flow velocity should be sonic to prevent transmission of lee-side or plenum noise into the shielded region (refs. 5 and 6)). The resulting large increases in the suction mass flow require a large increase in area of the main vacuum duct and a corresponding new design of the vacuum exhaust ducts for the 15 in. (38.1 cm) long model of reference 10.

The purpose of this note is to report the results of wind tunnel blockage tests of two sound shield models incorporating these new exhaust ducts. Tests were conducted in the Pilot Quiet Tunnel at Mach 5 with dummy versions of the exhaust ducts attached to the external housing of the sound shield models.

SYMBOLS

d	diameter
g	minimum gap spacing between rods
L	model length from leading edge to end of external housing (fig. 2)
M	Mach number
$\dot{m}$	mass flow
p	pressure
R	unit Reynolds number, $\frac{\rho u}{\mu}$
T	absolute temperature
u	velocity
δ^*	boundary layer displacement thickness
μ	viscosity coefficient
ρ	mass density
ω	inclination angle of external housing leading edge with respect to model centerline (see figure 2 (b))

Subscripts:

B	by-pass flow
box	tunnel vacuum box
cyl	cylinder
diff	diffuser
E	nozzle exit
I	isentropic
r	rod
s	inlet of shield model
sph	sphere
T	total flow
t	pitot tube values
V	vacuum
w	wall
o	isentropic stagnation conditions in wind tunnel
∞	free-stream conditions

APPARATUS AND TEST PROCEDURES

Wind Tunnel

Figure 1 (a) is a sketch of the settling chamber and vacuum box of the Langley Pilot Quiet Tunnel. The Mach 5 slotted nozzle is shown installed in the vacuum box which encloses the open jet test section of the facility. Details of the settling chamber components and disturbance measurements in the settling chamber and nozzle are available in reference 11. A description of the slotted nozzle and preliminary test data on the nozzle are also available in references 4 and 7.

The 12 in. (30.5 cm) diameter vacuum exhaust pipe shown in figures 1 (a) and 1 (b) is connected to a 60 ft. (18.3 m) diameter sphere which provides

the vacuum to operate the tunnel as a blow-down facility. An auxiliary vacuum pipe located at the forward upper surface of the vacuum box can be independently opened to the same sphere through the valve V-29 (figs. 1 (a) and 1 (b)). Data were generally obtained on the blockage models with this valve both open and closed. The physical locations of the valves and elbows in these vacuum lines are shown in figure 1 (b).

Data were obtained over a range of stagnation pressures from about 50 to 300 psia (34.5 to 206.8 N/cm^2). The stagnation temperature varied from about 630° to 700° R (350 to 390 K) for different runs but was held constant to within 15° R (8 K) during any given run. For these conditions, the unit Reynolds number at the nozzle exit ranged from approximately 2.4×10^6 to 13.8×10^6 per ft. (7.9×10^6 to 45.3×10^6 per m).

Models and Test Installation

Front, side, and rear view photographs of the two models with the dummy vacuum ducts attached are shown in figures 2 (a) and 2 (b). The first model (fig. 2 (a)), hereafter referred to as Model No. 1, consisted of a sharp leading edge, solid wall cylinder of 3 in. (7.62 cm) inside diameter and 18.65 in. (47.37 cm) long that was inserted into the same external housing used for the model of reference 10 and also for the second model tested during this investigation. Model No. 1 is intended to simulate the wind tunnel flow blockage of a new sound shield model with the same inside diameter (3 in. (7.62 cm)) and with $g/d = 0.16$. Model No. 2 is the sound shield of reference 10 but with the rods modified to provide $g/d = 0.12$. The rods can be seen in both the front and rear views of this model. The length of the basic model including the rods is 15 in. (38.1 cm) and the inside diameter at the sharp leading edge of the model is 4 in. (10.16 cm). The overall lengths, L, of the model housings are given in figures 2 (a) and 2 (b).

The dummy exhaust ducts were constructed of wood and were essentially the same for both models. A drawing of a typical duct is shown in figure 2 (c). The sharp leading edge of the ducts are swept back 63° from the nozzle inlet flow direction. The width of the ducts is 4 in. (10.16 cm) and the internal cross-sectional flow area of the actual ducts will be approximately 20.5 in.^{2} (132.3 cm^2).

Photographs of the models mounted in the open jet test section are shown in figure 3. The leading edges of both models are concentric with the laminar flow slotted nozzle and are located 1/4 in. (0.64 cm) forward of the nozzle exit. The right hand photographs show the diffuser bellmouth (see fig. 1 (a)).

By-Pass Mass Flow Ratios and Blockage Areas

The ratio of the by-pass mass flow (that is, the flow which by-passes the model) to the total mass flow in the tunnel is

$$\dot{m}_B/\dot{m}_T = \frac{\left(d_E - 2\delta^*_E\right)^2 - d_s^2}{\left(d_E - 2\delta^*_E\right)^2} \qquad (1)$$

where it has been assumed that the nozzle exit flow external to the boundary layer is uniform. The exit diameter of the nozzle $\left(d_E\right)$ is 5.082 in. (12.908 cm), so for $\delta^* = 0$, $\dot{m}_B/\dot{m}_T = 0.651$ and 0.381 for Model Numbers 1 and 2, respectively. The blockage (ref. 12) of the tunnel flow by a model may be defined as the ratio of the area determined from the projection onto the nozzle exit area of the model cross-sectional area, to the nozzle exit area. Therefore, for these tests, the model blockage is the same as the by-pass mass ratio for $\delta^* = 0$. Thus the flow blockage of Model No. 1 can be expected to be much larger than that of Model No. 2 not only because of the larger blockage area of Model No. 1 but also because most of the kinetic energy of the by-pass air for both models is probably dissipated before entering the

tunnel bellmouth and diffuser or the auxiliary vacuum line. Hence, the average total pressure of the flow entering the diffuser bellmouth or auxiliary vacuum line would be much lower for Model No. 1 than Model No. 2 and Model No. 1 will probably be more difficult to start than Model No. 2.

Detailed boundary layer calculations for the slotted nozzle are reported in reference 13. The value of δ_E^* obtained from reference 13 for the turbulent calculation with 3 percent turbulence level assumed and for p_o = 150 psia (103.4 N/cm^2) is 0.222 in (0.564 cm). For these conditions, $R_\infty \approx 6.7 \times 10^6$ per ft. (22×10^6 per m) and $\dot{m}_B/\dot{m}_T$ = 0.582 and 0.256 for Model Numbers 1 and 2, respectively. For comparison with these values, a measured value of δ^* from reference 14 for the "conventional" nozzle may be used. The length of this conventional nozzle (ref. 14) from the throat to the exit was 19.7 in. (50.0 cm). For $R_\infty = 10.4 \times 10^6$ per ft. (34.1×10^6 per m), $\delta_E^* = 0.15$ in (0.38 cm). The corresponding by-pass mass flow ratios, $\dot{m}_B/\dot{m}_T$, are 0.606 and 0.300 for Model Numbers 1 and 2, respectively. These results are summarized in the following table:

δ^*		Basis for δ^*	$\dot{m}_B/\dot{m}_T$ Model No.	
in.	cm		1.	2.
0	0	Inviscid	0.651	0.381
0.222	0.564	Ref. 13; slotted nozzle $R_\infty = 6.7 \times 10^6$ per ft (22×10^6 per m)	.582	.256
.150	.380	Ref. 14; conventional nozzle $R_\infty = 10.4 \times 10^6$ per ft (34.1×10^6 per m)	.606	.300

RESULTS AND DISCUSSION

Schlieren Photographs

Schlieren photographs were obtained to provide qualitative information about the flow behavior. Figure 4 shows typical schlieren photographs of the flow at the exit of the two models for R_∞ values at the lower end of the range and also for intermediate values of R_∞. The time exposures for these photographs (given in the figure) are such that any unsteady disturbances would tend to be smeared out. Hence, for Model No. 1 (fig. 4 (a)), the upper and lower shocks are evidently unsteady and indicate a partial breakdown of supersonic flow near the outer edges of the exit flow. However, the formation of steady shocks on the pitot tubes which are near the center of the flow, indicates the central region of the flow was at least partially started.

The exit shocks for Model No. 2 (fig. 4 (b)) appear to be steady indicating the flow in this model was probably fully started. It is of interest to note that the inside exit shocks for Model No. 2 are probably caused by separation of the flow at the end of the rods and reattachment on the exit cylinder (which has a raduis of 2.03 in. (5.16 cm)) as indicated in the left-hand photograph of figure 4 (b). To evaluate these qualitative indications of the flow behavior, it is necessary to examine measurements of static and pitot pressures.

Nozzle Wall Static Pressures

Four static pressure orifices were installed upstream of the nozzle exit at intervals of 1/4 in. (0.635 cm) from the exit. When shock disturbances are present near the exit of the nozzle, these pressures increase significantly above the level for undisturbed flow (at $M_\infty \approx 4.9$), indicating at least some breakdown of the supersonic exit flow as well as the possibility of disturbances entering the flow inside the models.

The measured nozzle static pressures, normalized by the stagnation pressure are presented in figure 5 for both models. By comparison of these normalized pressures with the level for $M_\infty = 4.9$, indicated in the figure, it is apparent that the exit flow for Model No. 1 (fig. 5(a)) was probably not started and that large disturbances would enter the interior flow region in the model except possibly at the lowest unit Reynolds number where the nozzle flow was more nearly started. (Fully started flow at this lowest unit Reynolds number may have been prevented by the high sphere pressure, to be shown later.) When the vacuum valve V-29 (see fig. 1(b)) was closed, this flow breakdown condition was intensified as indicated by the increase in static pressure at $R_\infty = 4.71 \times 10^6$ per ft (15.50×10^6 per m). However, the static pressure levels for Model No. 2 (fig. 5(b)) indicate that the flow was started over the whole range of R_∞ and remained started at $R_\infty = 9.25 \times 10^6$ per ft (30.35×10^6 per m) even when V-29 was closed. The increase in pressure ratio at the orifice closest to the exit for the data with Model No. 2 is caused by the high box pressures and indicates the presence of some relatively weak shock disturbances. These disturbances presumably could not enter the flow inside the model because the model leading edge is 1/4 in. (0.635 cm) upstream of the nozzle exit and 1 in. (2.54 cm) smaller in diameter than the nozzle exit.

Vacuum Box Pressures

Static pressures measured in the vacuum box (see fig. 1) of the tunnel are presented in figure 6 where p_{box}/p_o ratios are plotted against free stream unit Reynolds number. Comparison of the results obtained with the models in place to data obtained with no models in the tunnel (open tunnel) shows that Model No. 1 caused large increases in box pressure up to 10 times the open tunnel values with V-29 closed. However, with Model No. 2 in the test section, only a slight increase in box pressure occurred when V-29 was closed. On the basis of the limited data presented so far, indicating that the flow was not started in Model No. 1 but probably was started in Model No. 2, it may be tentatively concluded

from figure 6 that the vacuum box pressure ratios should be maintained at levels of about 0.006 or less to maintain a started flow condition. To further assess flow conditions, the pitot pressures at the model exit and static pressures inside the models must be examined.

Pitot Pressures at Model Exits

Mean pitot pressures were measured at the model exits with the small three-tube rake which can be seen in the schlieren photographs of figure 4. The pitot tubes were made of steel tubing of 0.021 in (0.053 cm) outside diameter and 0.013 in.(0.033 cm) inside diameter. The tubes were spaced at 0.25 in. (0.635 cm) apart on the rake and the center tube was located on the model centerline. The ratios of the measured pitot pressures to the settling chamber stagnation pressure are presented in figure 7. Again, by comparison with the open tunnel values, it may be concluded that the flow in the vicinity of the rake was started for Model No. 1 (fig. 7 (a)) only at the highest unit Reynolds number. At the next lowest unit Reynolds number of $R_\infty = 6.75 \times 10^6$ per ft. (22.15×10^6 per m) the flow was probably not fully started. The region of started flow at this value of R_∞ was apparently limited to a small region in the center of the model as shown by the right-hand photograph of figure 4 (a). At the two lower unit Reynolds numbers, the large increases in p_t/p_o indicate the flow was not started.

For Model No. 2, the flow is believed to be started at the three highest unit Reynolds numbers but with some residual disturbances and nonuniform flow present. The flow is apparently not started at the lowest unit Reynolds number. This latter result may be related to the observed increases in nozzle wall static pressures at the lowest unit Reynolds number (see fig. 5 (b)). Closer examination of the corresponding schlieren photograph in figure 4 (b)

reveals that the upper shock may be somewhat unsteady as indicated by the blurred image of this shock. Thus, on the basis of these pitot pressure data as well as the schlieren and nozzle static pressure data, it may be concluded that the flow in Model No. 2 was not fully started at the lowest unit Reynolds number.

The nominal by-pass mass flow ratios were 0.6 and 0.3 for Model Numbers 1 and 2, respectfully (see table on pg. 7). Hence on the basis of the data presented thus far and the assumption that the by-pass mass flow ratio from equation (1) is the dominant criterion for obtaining started flow, it may be concluded that the by-pass mass flow ratios for a wind tunnel sound shield with an external housing and vacuum ducts similar to those tested here would have to be maintained at about 0.25 or less to insure starting the flow over the entire present range of unit Reynolds numbers. As an example, if d_E = 20 in (50.8 cm), the sound shield diameter would have to be about 17.3 in (43.9 cm) or larger in diameter.

It should be emphasized, however, that suction mass flow through the rod gaps such as required on an actual sound shield (see ref. 10) could not be simulated during the present tests. Data reported in reference 10 indicated that this suction mass flow tended to alleviate marginal choked flow conditions. Consequently, the above minimum values of by-pass mass flow ratios could probably be increased slightly. It should also be emphasized that the by-pass flow ratios could probably be significantly increased (which would allow the use of a smaller shield) by improvements in external "streamlining" to reduce the aerodynamic drag of the external housing and ducts of the models. Another proven technique to start large blockage models is the use of an external shroud (see ref. 12) which reduces the total pressure losses of the by-pass flow.

Further tests would be required to develop and verify these techniques for the present models.

Model Static Pressures

Static pressure orifices were installed inside the 3 in. (7.62 cm) diameter cylinder of Model No. 1 and along the inside of the rods facing the interior core flow on Model No. 2. The measured pressures normalized with the tunnel stagnation pressure, are plotted against distance from the leading edge in figure 8. For Model No. 1 (fig. 8 (a)), the pressures increase toward the rear of the model indicating that the high box pressures (see fig. 6) are probably causing separation in this region. The schlieren photographs (fig. 4 (a)) also provide evidence of flow separation at the rear of this model.

The static pressures on the rods of Model No. 2 (fig. 8 (b)) appear to be higher than might be expected ($p_\infty/p_o \approx 0.0021$ for $M_\infty = 4.9$) based on most of the data presented so far. Examination of the assembled model indicated that a small clearance was present between the leading edge of the shells which support the ducts and the model housing at the shoulder (see fig. 3 (b)). Since the pressure at this shoulder would be considerably higher than the free-stream static pressure, it is believed that some leakage of high pressure air into the model in the region around the outside of the rods occurred. If so, the higher than expected pressures in fig. 8 (b) were caused by this internal "pressurization" of the model and blowing of this air through the rod gaps into the internal core flow region. Indeed, this leakage of high pressure air into the model may be the cause for the large pitot pressures measured at the exit of Model No. 2 at the lowest unit Reynolds number (see fig. 7 (b)).

Diffuser Static Pressures

To determine if the vacuum sphere pressures were approaching values too high to maintain flow for any of the data from runs included in this report, the pressures in the sphere (normalized by the tunnel stagnation pressure) recorded at the same time as all other data for a given run are plotted in figure 9. The normalized static pressures in the 12 in. (30.5 cm) diameter tunnel exit pipe at about 53 in (134.6 cm) downstream of the end of the vacuum box (see fig. 1 (b)) are also plotted in this figure for comparison. (This pressure orifice was about 26 in. (66 cm) downstream of the end of the diffuser pipe.) Finally, the variations of p_{box}/p_o from fig. 6 are also included in this figure. Comparison of these pressures for the runs with Model No. 1 show that the box pressures were higher than the sphere pressures at the three highest unit Reynolds numbers. It follows that improved flow would be obtained with V-29 open at the higher Reynolds numbers. At the lowest unit Reynolds number, flow breakdown has evidently occurred due to the high sphere pressure.

With Model No. 2, the differences between box pressure and sphere pressure are smaller so that the main diffuser was able to carry most of the mass flow. At the three highest Reynolds numbers, the sphere pressure was always higher than the diffuser static pressure indicating that pressure recovery occurred downstream of the diffuser static orifice station.

CONCLUDING REMARKS

Two sound shield models with vacuum exhaust ducts have been tested for wind tunnel flow blockage at Mach 5. The smallest model, which is a solid wall cylinder designed to simulate the flow blockage of a new sound shield of 3 in. (7.62 cm) inside diameter, could not be started except at the two highest test Reynolds

numbers where only the central region of the flow was started. The other model has an inside diameter of 4 in. (10.16 cm) and consists of a cylindrical array of nearly parallel rods. This model is the same sound shield model tested previously with smaller gaps between the rods. The internal flow of this model was started except at the lowest unit Reynolds number when leakage of high pressure air into the plenum region around the rods and subsequently from the plenum through the gaps between the rods into the internal core flow was probably responsible for the flow breakdown.

The ratios of the by-pass mass flow around the models to the total mass flow in the tunnel was approximately 0.6 for the first model and 0.3 for the second model. Therefore, if the by-pass mass flow ratio is the dominant criterion for obtaining started flow, this ratio must be somewhat smaller than 0.3 to insure that the flow can be started over the entire Reynolds number range from about 2.5×10^6 per ft (8.2×10^6 per m) to 14×10^6 per ft (45.9×10^6 per m) through a sound shield with vacuum ducts similar to those tested. It follows that without significant improvements in the external aerodynamic streamlining of the sound shield, and/or reductions in blockage area of the external housing and ducts, or by the use of an external shroud to reduce losses in total pressure of the by-pass air, the inlet diameter of the shield cannot be reduced below the limits determined by this by-pass mass flow ratio.

REFERENCES

1. Laufer J.: Aerodynamic Noise in Supersonic Wind Tunnels. J. Aero. Sci., vol. 28, no. 9, Sept. 1961, pp. 685-692.

2. Pate, S. R.; and Schueler, C. J.: Radiated Aerodynamic Noise Effects on Boundary Layer Transition in Supersonic and Hypersonic Wind Tunnels. AIAA Journal, vol. 7, no. 3, Mar. 1969, pp. 450-457.

3. Stainback, P. C.; Fischer, M. C.; and Wagner, R. D.: Effects of Wind-Tunnel Disturbances on Hypersonic Boundary-Layer Transition. Parts I and II. AIAA Paper No. 72-181, 1972.

4. Harvey, W. D.; Stainback, P. C.; Anders, J. B.; and Cary, A. M.: Nozzle Wall Boundary Layer Transition and Free Stream Disturbances at Mach 5. AIAA Journal, Vol. 13, No. 3, March 1975, pp. 300-306.

5. Beckwith, Ivan E.; and Bertram, Mitchel H.: A Survey of NASA Langley Studies on High-Speed Transition and the Quiet Tunnel. NASA TM X-2566, July 1972.

6. Harvey, W. D.; Berger, M. H.; and Stainback, P. C.: Experimental and Theoretical Investigation of a Slotted Noise Shield Model for Wind Tunnel Walls. AIAA Paper No. 74-624, 1974.

7. Beckwith, I. E.: Development of a High Reynolds Number Quiet Tunnel for Transition Research. AIAA Journal, Vol. 13, No. 5, March 1975, pp. 300-306.

8. Harvey, W. D.: Effect of Rod Gap Spacing on a Suction Panel for Laminar Flow and Noise Control in Supersonic Wind Tunnels. Masters Thesis. Old Dominion University, May, 1975.

9. Stainback, P. C.; Harvey, W. D.; and Srokowski, A. J.: Effect of Suction Slot Width on Transition and Noise Attenuation of a Flat Sound Shield in a Mach 6 Wind Tunnel. NASA TN D-8081, 1975.

10. Beckwith, I. E.; Srokowski, A. J.; Harvey, W. D.; and Stainback, P. C.: Design and Preliminary Test Results at Mach 5 of an Axisymmetric Slotted Sound Shield. NASA TM X-72679, June 1975.

11. Anders, J. B.; Stainback, P. C.; Keefe, L. R.; and Beckwith, I. E.: Sound and Fluctuating Disturbance Measurements in the Settling Chamber and Test Section of a Small Mach 5 Wind Tunnel. Paper presented at the 6th Int. Cong. on Inst. in Aerospace Simulation Facilities, Ottawa, Canada, September 22-24, 1975.

12. Molloy, J. K.; Mackley, E. A.; and Keyes, J. W.: Effect of Diffusers, Shrouds, and Mass Injection on the Starting and Operating Characteristics of a Mach 5 Free Jet Tunnel. NASA TN D-6377, Sept., 1971.

13. Kreskovsky, J. P.; Shamroth, S. J.; and McDonald, H.: Parametric Study of Relaminarization of Turbulent Boundary Layers on Nozzle Walls. NASA CR-2370, June 1974.

14. Stainback, P. C.; Anders, J. B.; Harvey, W. D.; Cary, A. M., and Harris, J. E.: An Investigation of Boundary-Layer Transition on the Wall of a Mach 5 Nozzle. Parts I and II. AIAA Paper No. 74-136, 1974.

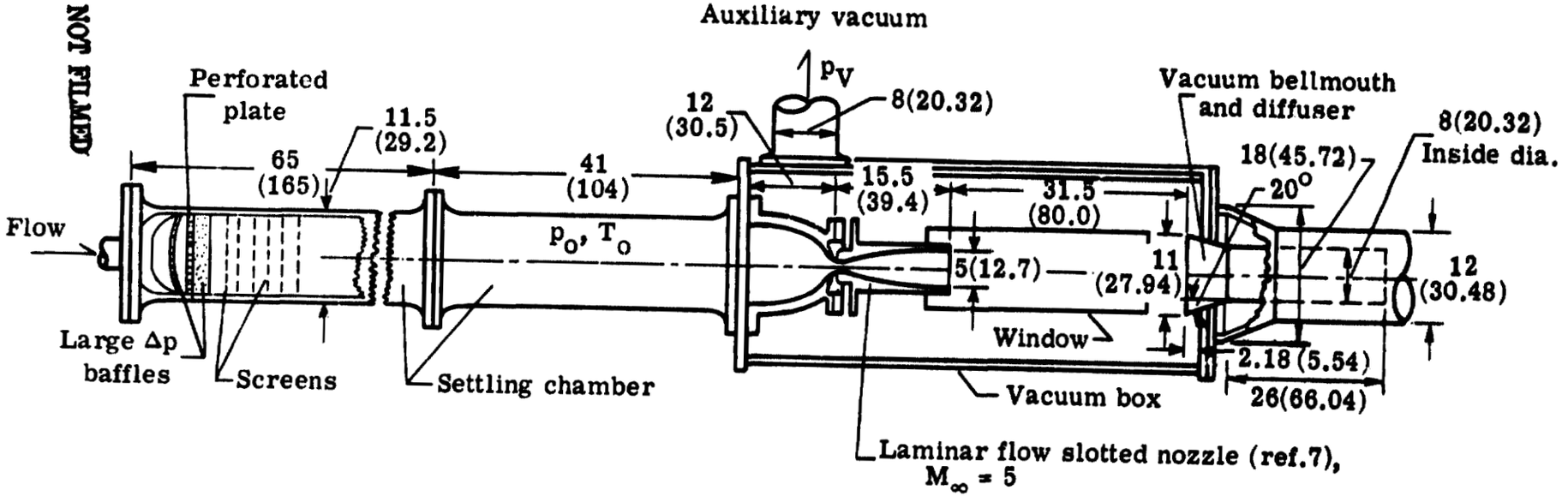

(a) Side view of settling chamber and test section.

Figure 1.- Schematic sketch of Pilot Quiet Tunnel. All dimensions in inches (cm).

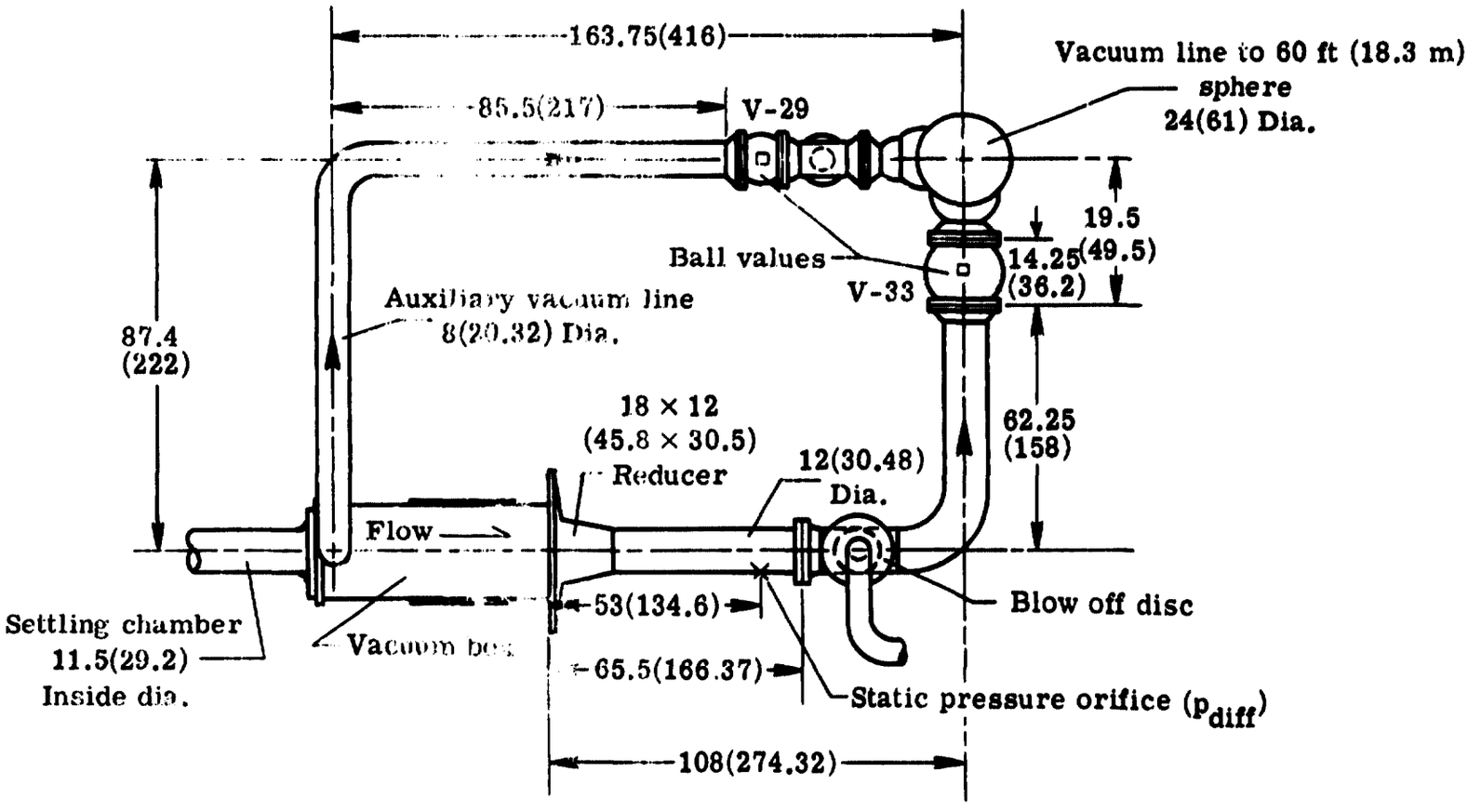

(b) Plan view of vacuum lines to 60 ft (18.3 m) sphere.

Figure 1.- Concluded.

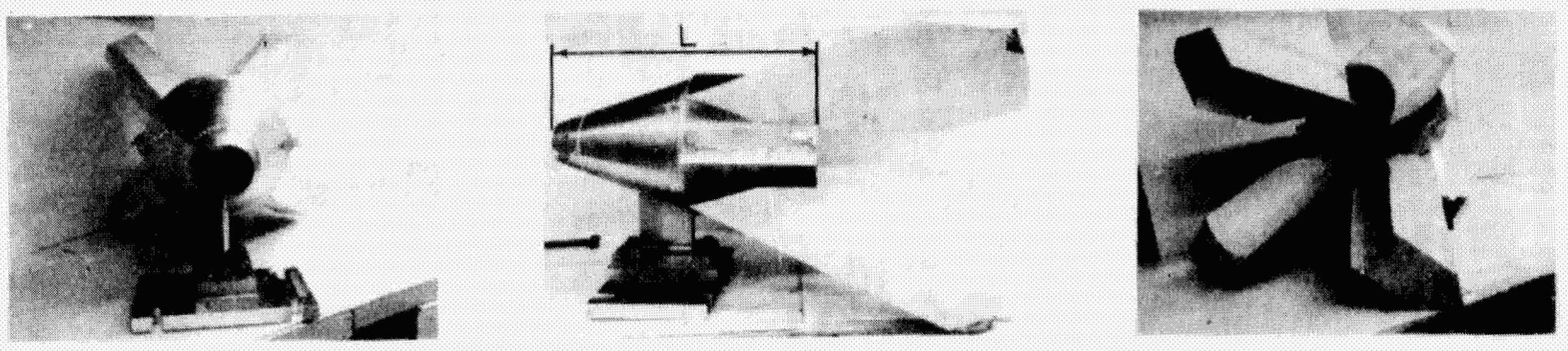

Front Side Rear

(a) Model no. 1; 3 in. (7.62 cm) inside diameter, L = 18.65 in. (47.37 cm).

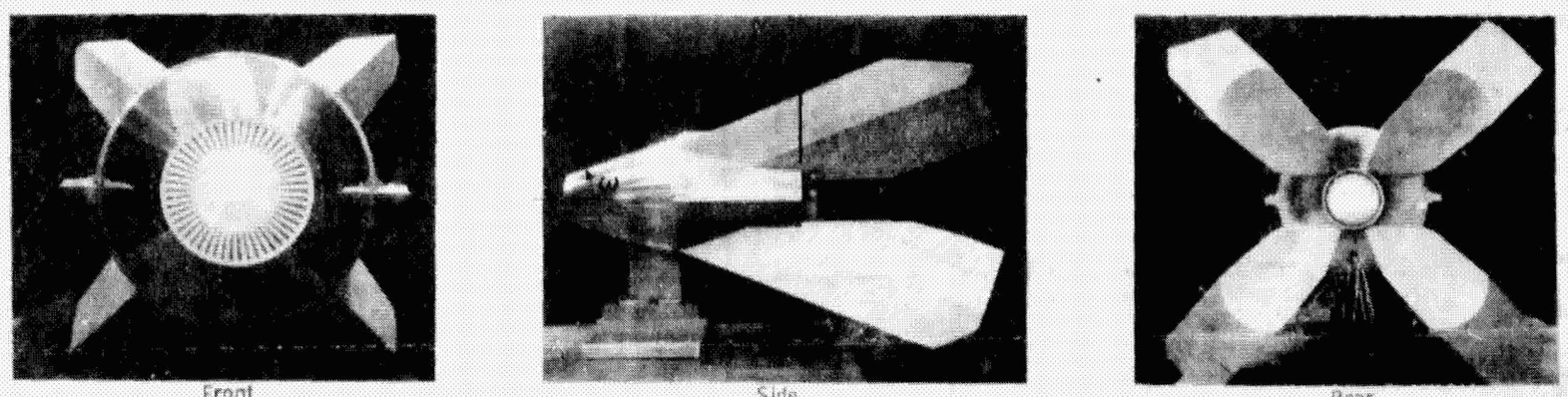

Front Side Rear

(b) Model no. 2; 4 in. (10.16 cm) inside diameter, L = 17.27 in. (43.87 cm).

Figure 2. Photographs of the two models with dummy exhaust ducts attached. Dimensions of model housing: maximum outside diameter = 10.5 in. (26.67 cm); leading edge housing angle $\omega = 20^0$.

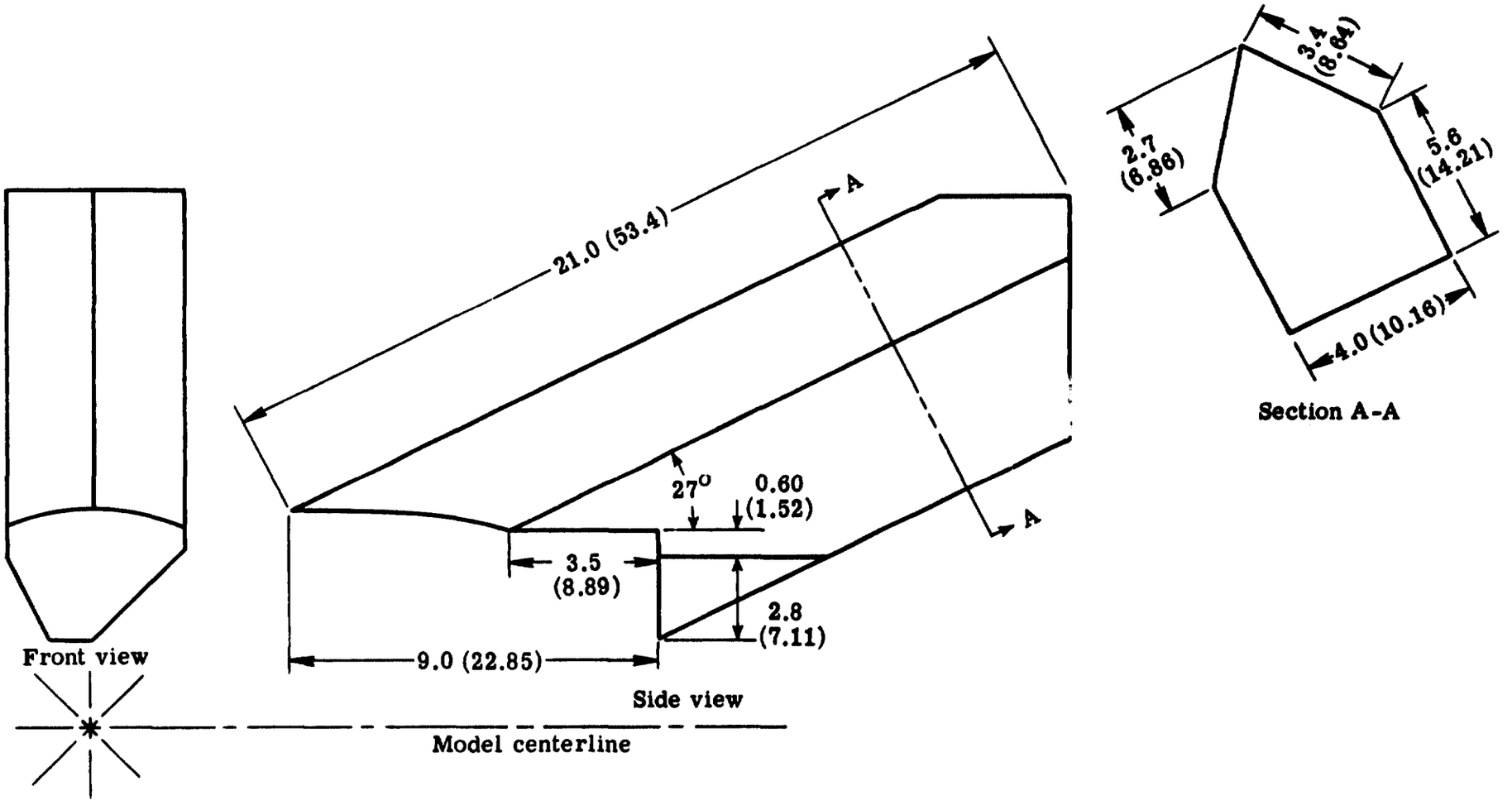

(c) Drawing of typical dummy duct. All dimensions in inches (cm).

Figure 2.- Concluded.

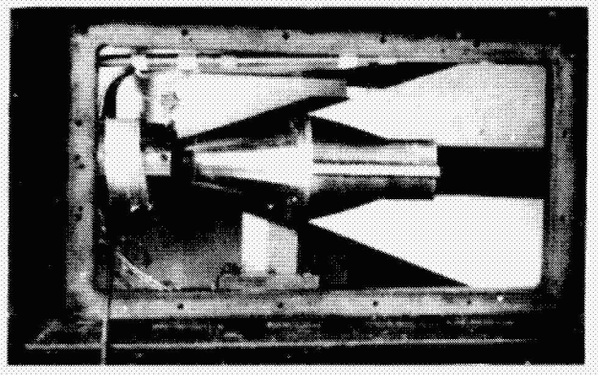

Side view

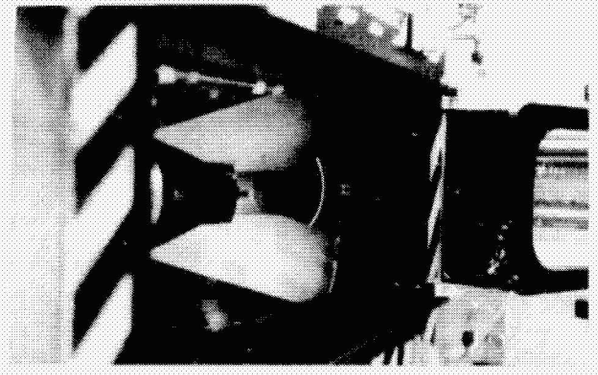

Three-quarter front view

(a) Model no. 1.

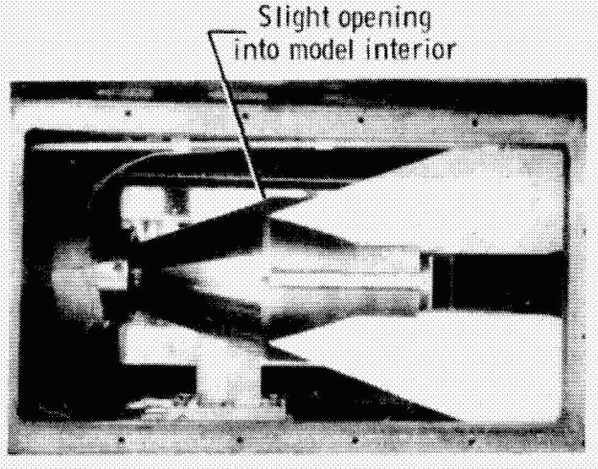

Side view

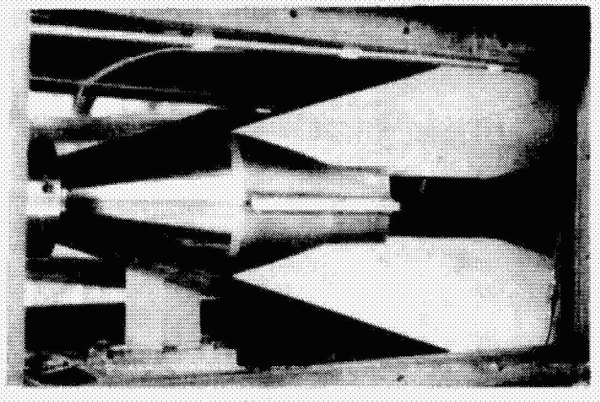

Angled front view

(b) Model no. 2.

Figure 3.- Photographs of models mounted in test section.

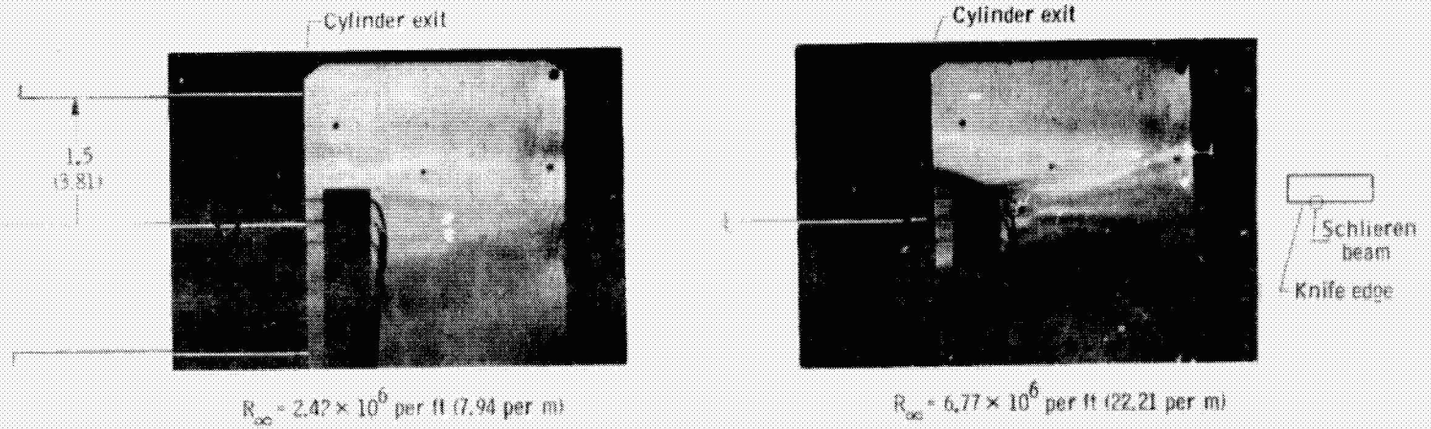

$R_\infty = 2.42 \times 10^6$ per ft (7.94 per m) $R_\infty = 6.77 \times 10^6$ per ft (22.21 per m)

(a) Model no. 1 ; 4 sec exposure.

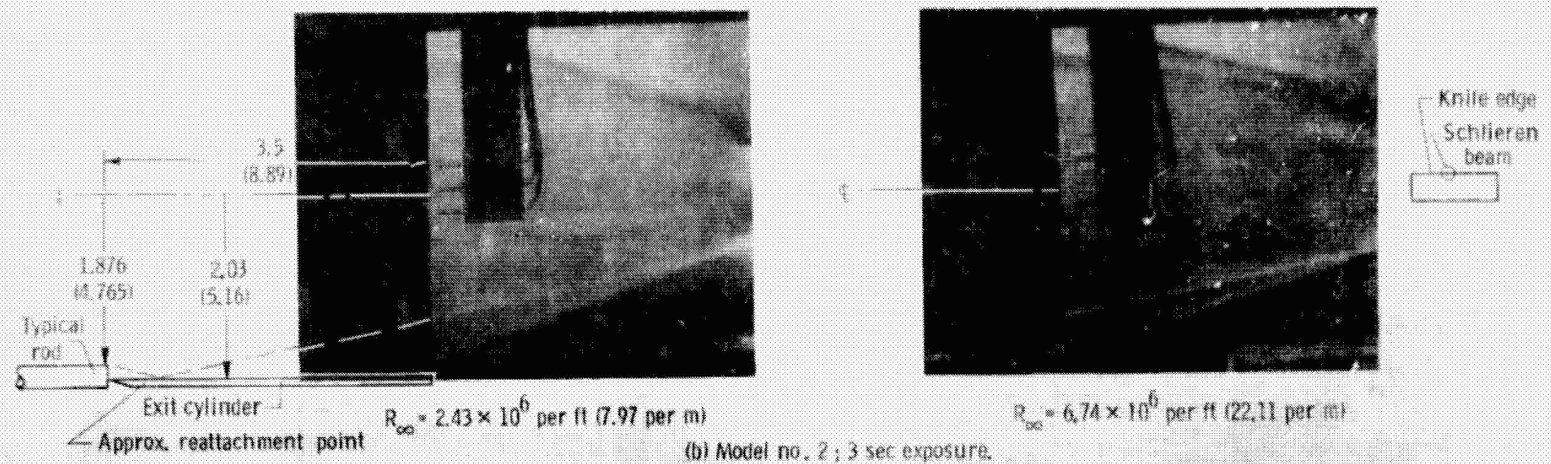

$R_\infty = 2.43 \times 10^6$ per ft (7.97 per m) $R_\infty = 6.74 \times 10^6$ per ft (22.11 per m)

(b) Model no. 2 ; 3 sec exposure.

Figure 4.- Schlieren photographs of flow at exit of models. Dimensions in inches (cm).

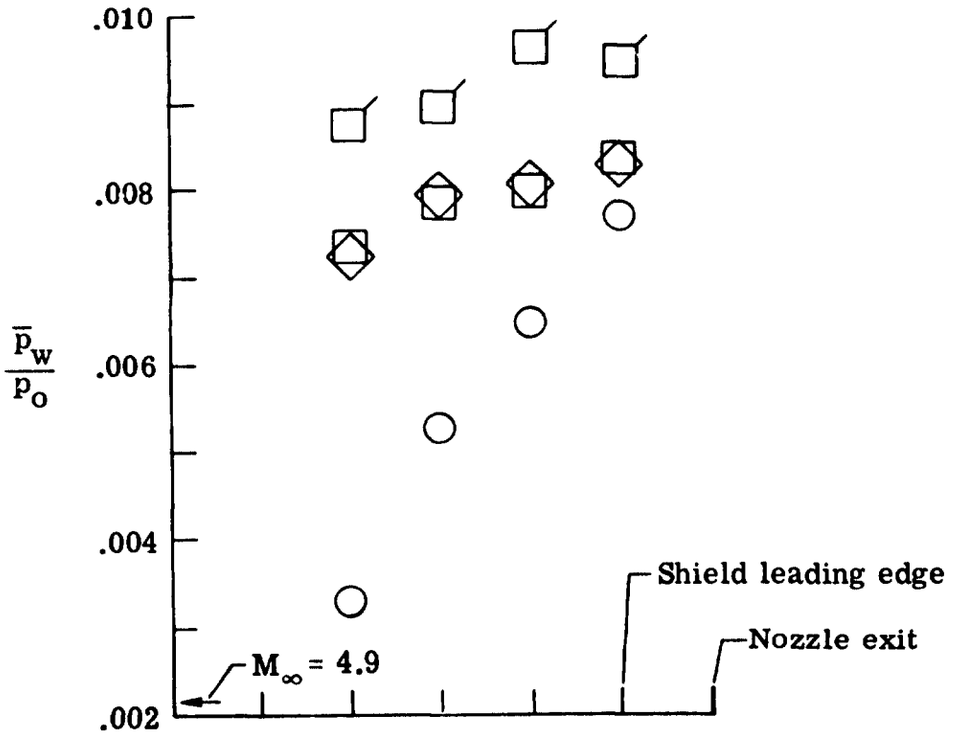

(a) Model no. 1.

$R_\infty \times 10^{-6}$

	per ft	per m
○	2.41	7.90
□	4.71	15.50
◇	6.78	22.22

Flagged symbols: V-29 closed

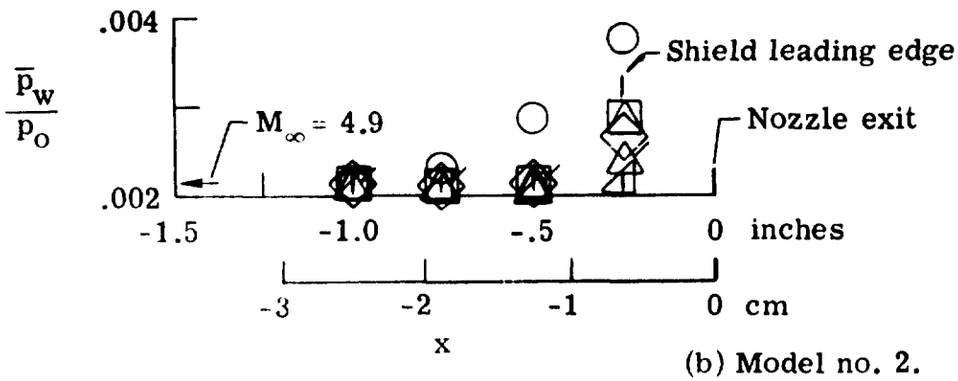

(b) Model no. 2.

$R_\infty \times 10^{-6}$

	per ft	per m	
○	2.43	7.98	
□	4.74	15.55	
◇	6.74	22.10	
△	9.10	29.90	
◁	13.67	44.90	
△	9.25	30.35	V-29 closed

Figure 5.- Distributions of nozzle wall static pressures.

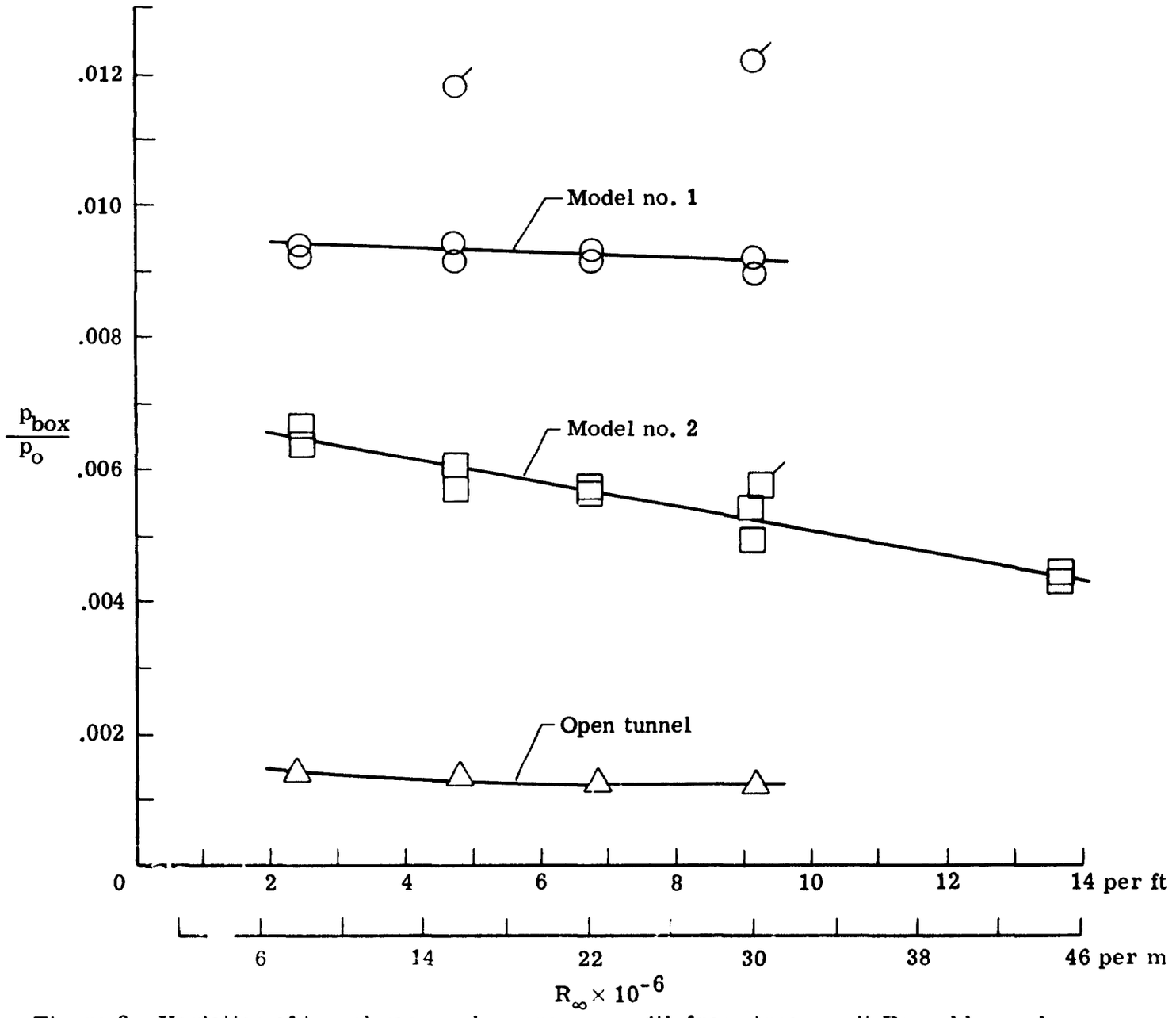

Figure 6.- Variation of tunnel vacuum box pressure with free stream unit Reynolds number. Flagged symbols for V-29 closed.

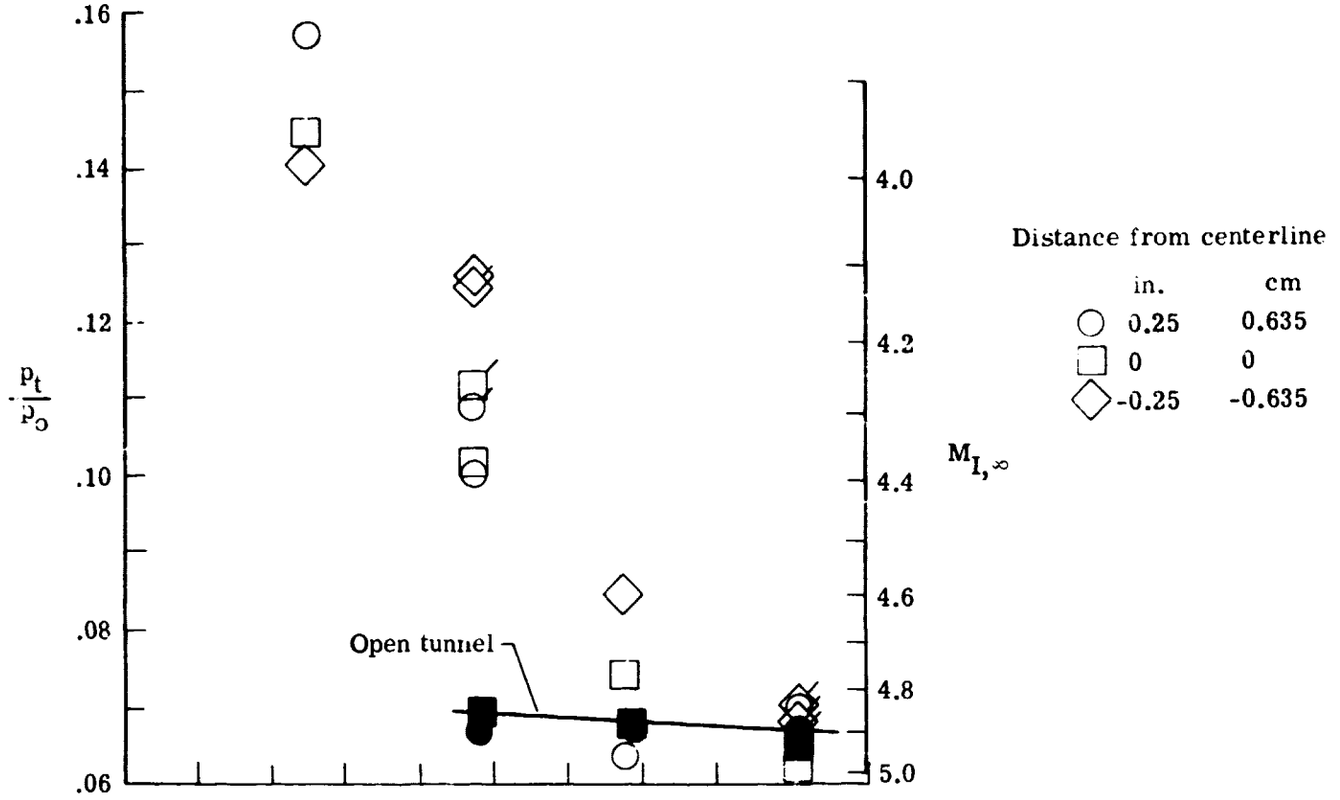

(a) Model no. 1.

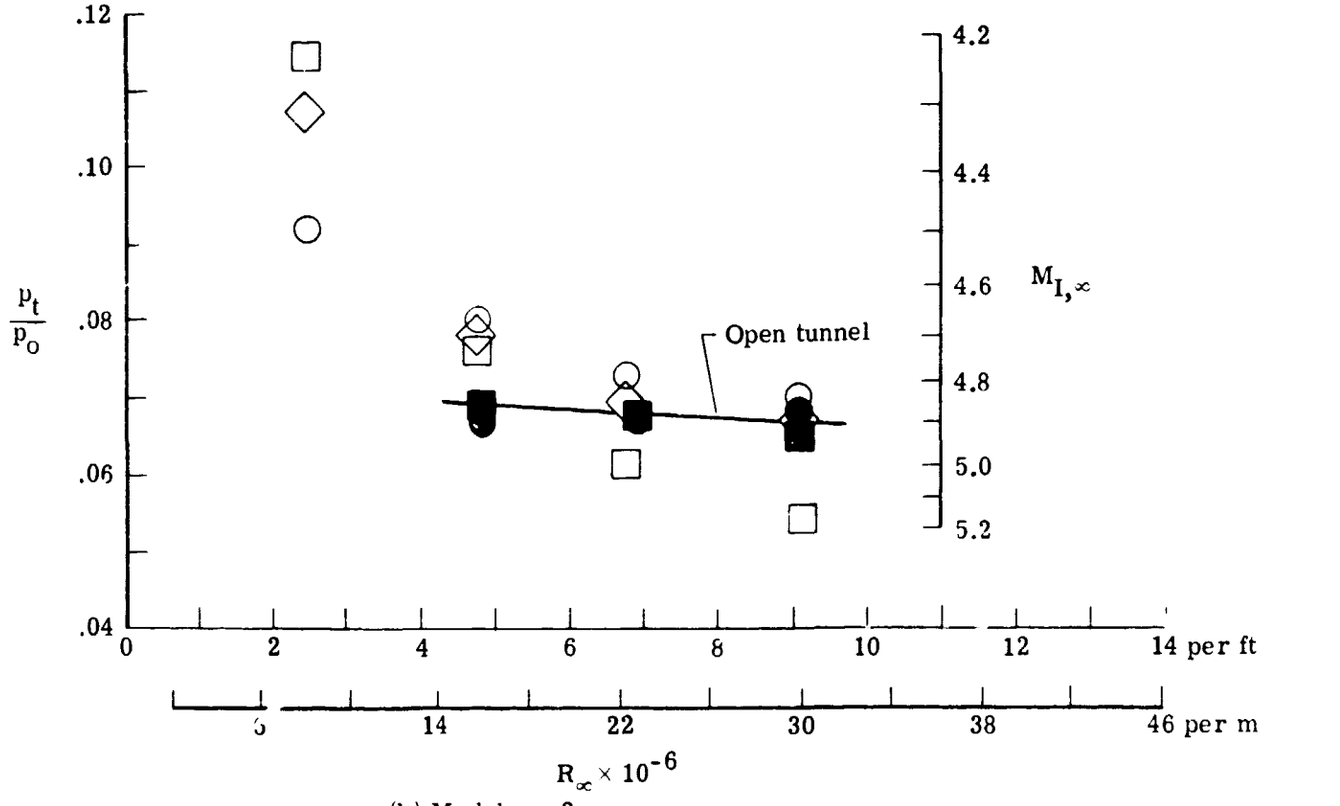

(b) Model no. 2.

Figure 7.- Variation of mean pitot pressure at model exits with free stream unit Reynolds number.

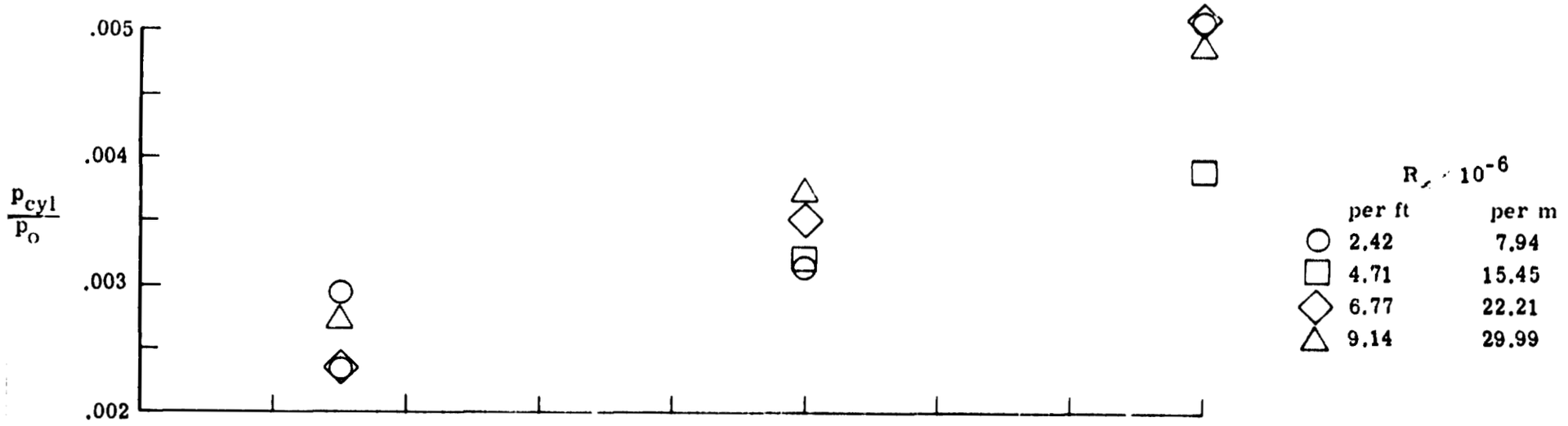

(a) Model no. 1.

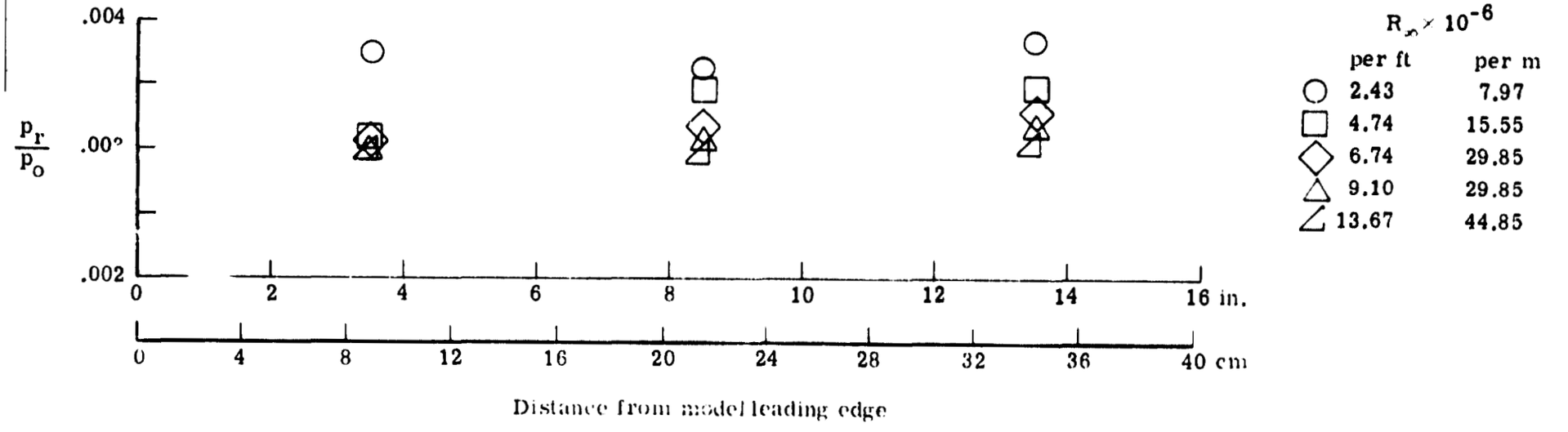

(b) Model no. 2.

Figure 8.- Distribution of static pressures inside the models.

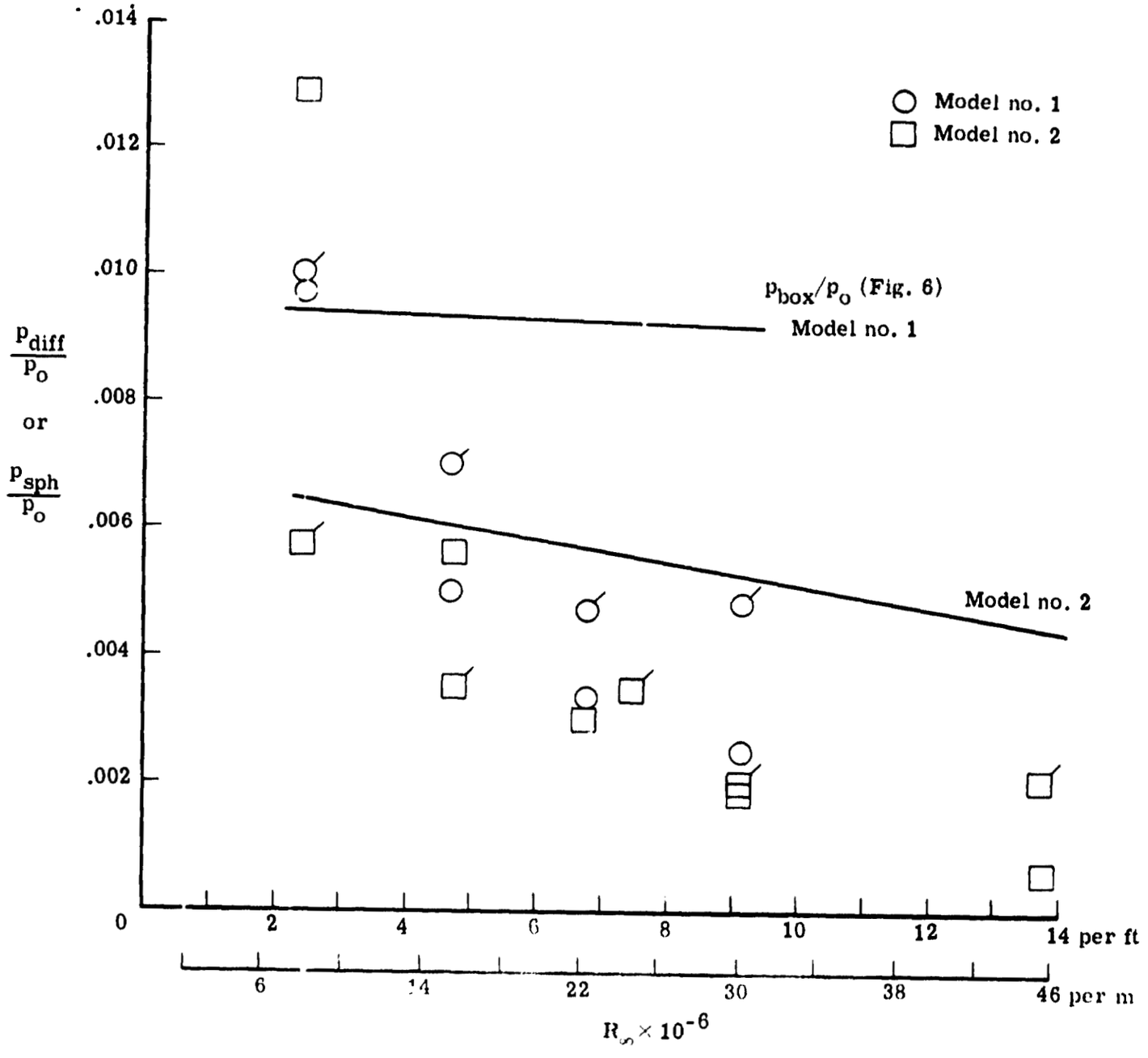

Figure 9.- Diffuser static pressure variation with R_∞ and sphere pressures, denoted by flagged symbols, recorded at same time as all other data for a given run.